



RESEARCH MEMORANDUM

A STUDY OF LIQUID BORIC OXIDE PARTICLE GROWTH RATES
IN A GAS STREAM FROM A SIMULATED
JET ENGINE COMBUSTOR

By Paul C. Setze

Lewis Flight Propulsion Laboratory
Cleveland, Ohio

NATIONAL ADVISORY COMMITTEE
FOR AERONAUTICS
WASHINGTON

April 30, 1957
Declassified April 15, 1958

NATIONAL ADVISORY COMMITTEE FOR AERONAUTICS

RESEARCH MEMORANDUM

A STUDY OF LIQUID BORIC OXIDE PARTICLE GROWTH RATES IN A GAS STREAM
FROM A SIMULATED JET-ENGINE COMBUSTOR

By Paul C. Setze

SUMMARY

It was experimentally determined that the liquid boric oxide particles leaving a jet-engine combustor that is burning a boron-containing fuel will have diameters of 1×10^{-5} to 2.0×10^{-5} centimeter. For this size range the particle drag coefficient and heat-transfer coefficient are essentially infinite. These results may be applied to any boron-containing fuel.

A study of boric oxide deposition mechanisms is included and suggestions for decreasing deposition rates given.

INTRODUCTION

Boron hydrides are being tested as aircraft fuels because their heating values are as much as 65 percent higher than those of hydrocarbons. They differ from conventional fuels in that, at the usual jet-engine operating temperatures, one of the combustion products, boric oxide (B_2O_3), appears as a viscous liquid. The liquid boric oxide can produce performance losses by collecting on critical engine surfaces and "spoiling" the flow of combustion gases.

In order to calculate the performance of the boron fuels, it is necessary to know the growth rate of the liquid particles in the exhaust gases (ref. 1). When the particle diameter is less than 2.2×10^{-6} centimeter, 3 percent or more of the heat of vaporization is in the form of surface energy. When the particle consists of a single molecule, the entire heat of vaporization (1994 Btu/lb, ref. 2) appears as this surface energy and is not transferred to the gas stream. However, if the particle diameter exceeds 3×10^{-4} centimeters, the entire heat of vaporization of the boric oxide that was previously held by the surface energy of the particles is absorbed by the working fluid, but the particles are so large that they cease to be in temperature and velocity equilibrium

with the gas stream. Reference 1 shows that for pentaborane fuel (B_5H_9) at a flight Mach number of 3.25 and a combustion temperature of $2200^{\circ} R$ a maximum theoretical gain of 250 seconds in engine impulse is attainable if the liquid boric oxide particles are in the range of infinite drag and infinite heat transfer (diameters less than 3×10^{-4} cm). Therefore, it would be desirable for the particle diameters to fall between 2.2×10^{-6} and 3×10^{-4} centimeter where less than 3 percent of the latent heat of vaporization is held by surface energy and the particles have essentially infinite drag coefficient and heat-transfer coefficient.

Additional losses can occur when the liquid boric oxide deposits on engine surfaces. If the surface temperature is below the freezing point of boric oxide, large obstructions to flow may result. The manner in which boric oxide deposits and the techniques for reducing deposition rates are strongly dependent on particle size.

Observations previous to this time (ref. 3) have indicated that the liquid boric oxide is in the form of very small spherical droplets that grow in volume as a function of time. These observations were purely qualitative, however, and no accurate estimate of the particle size or rate of growth was made. Along with these very scant experimental observations, an attempt (ref. 3) was made to correlate the growth of liquid boric oxide particles with some of the parameters in a previous theoretical work on the coagulation of colloids by Smoluchowski (ref. 4). In addition to this, a number of theoretical and experimental papers have been published on the coagulation of aerosols, but these systems do not simulate the particle growth process in a jet-engine combustor.

Because of the status of this field of particle growth, an experimental and theoretical study of particle growth was initiated at the NACA Lewis laboratory. The two specific objectives of this program were: (1) establishment of particle size so that accurate quantitative values of performance parameters for boron fuels can be calculated; and (2) determination of size and motion of liquid boric oxide particles so that the mechanism of deposition can be better understood.

The range of variables considered in this investigation was representative of turbojet-engine operating conditions: pressure, 1 to 1.5 atmospheres; inlet temperature, $580^{\circ} R$; outlet temperature, 1260° to $2260^{\circ} R$; and particle growth time, 2.5 to 30.0 milliseconds. In all cases the combustor outlet temperature was at least $1800^{\circ} R$ lower than the saturation temperature of the liquid boric oxide. The boric oxide vapor-pressure data are taken from reference 5.

The theoretical work took the form of a general particle growth equation based on statistical collisions between particles. This equation was then applied to the two particle size ranges of interest:

(1) particle diameters less than 2.2×10^{-6} centimeter, where considerable energy is in the form of surface energy; and (2) particle diameters greater than 2.2×10^{-6} centimeter, where negligible energy is in the form of surface energy.

The experimental program was performed in a 4-inch connected-pipe facility using pentaborane (B_5H_9) fuel. At a predetermined station downstream of the fuel injector, a portion of the exhaust gas entered a sampling probe, where it was rapidly quenched with liquid nitrogen to a temperature well below the freezing temperature of boric oxide. The now solid boric oxide particles were collected and analyzed for size, shape, and composition.

To show the applicability of the results obtained in the 4-inch connected-pipe facility to turbojet engine applications, a single test was conducted using the single J47 combustor of reference 6.

The results of both the theoretical and experimental program are reported herein.

SYMBOLS

The following symbols are used in this report:

A	area, sq cm
C	concentration, g/cc
c_p	specific heat, cal/(g)(°K)
D	diameter, cm
E	energy, ergs
f/a	fuel-air ratio
$(f/a)^*$	stoichiometric fuel-air ratio
K	diffusion coefficient, sq cm/sec
k	constant defined by equation (22)
k'	constant defined by equation (14)
l	length, cm
M	molecular weight, g/mole

m	mass of material diffused, g/sec
N	Avogadro's number, 6.02×10^{23}
N_C	number of collisions
n	total number of particles
n_m	number of moles
n_p	number of particles per unit volume of gas
n'_p	number of particles per unit mass of particles
p	pressure, dynes/sq cm
R	universal gas constant, dyne-cm/(mole)(°K)
T	absolute temperature, °K
u	velocity, cm/sec
v	volume, cc
w	mass, g
X	mole fraction
x	weight fraction
δ	diffusion boundary-layer thickness, cm
λ	latent heat of vaporization, cal/g
ξ	molecular velocity, cm/sec
ρ	density, g/cc
σ	surface tension, dyne/cm
τ	time, sec
ϕ	equivalence ratio, dimensionless

Subscripts:

F flame

f final
g gaseous phase
L liquid phase
0 at time zero
p particle
s mainstream
T total
w wall
 τ at time τ

THEORY

Theoretical Model and Preliminary Assumptions

The system under consideration is that of an air stream flowing through a duct of constant cross-sectional area. A boron-containing fuel is added and the resultant fuel-air mixture burned. Gaseous boric oxide is formed in the flame zone. Additional air is added and cools the flowing stream to a temperature below the saturation temperature of boric oxide. (It is assumed that the boric oxide concentration is such that a negligible amount of boric oxide vapor will be present.) The boric oxide molecules can now collide and remain together forming a discrete liquid particle. These liquid particles will continue to collide and grow in size as a result of these collisions.

The following assumptions regarding the system are made:

- (1) There is a range of conditions over which the collision of two or more liquid boric oxide particles will result in the formation of one larger particle (see refs. 7 and 8).
- (2) The particles are spherical.
- (3) The particles are evenly distributed across the duct cross section.
- (4) At any one station in the combustor, the particle diameter range is sufficiently narrow so that an average particle diameter may be chosen that expresses the particle diameter term to be used in the growth equation (see ref. 9).

- (5) The particle may be treated as a large gas molecule.
- (6) The liquid droplets are treated as point particles.

General Equations

Assume that a particle of diameter D_p and velocity u_p is moving along a linear path. The moving particle now passes through a group of identical particles randomly distributed and at rest. The moving particle will collide with any other particle whose center lies within the distance D_p of the path along which it travels. During a unit of time τ , the distance the particle travels is $u_p\tau$.

The number of collisions in time τ is equal to the number of particles whose centers lie within a cylinder of volume equal to $\pi D_p^2 u_p \tau$. If n_p is the number of particles per unit volume of gas, the number of collisions made by the moving particle in time τ is equal to $n_p \pi D_p^2 u_p \tau$.

In reality all the particles are moving in random directions with average velocity u_p . According to Loeb (ref. 10), the velocity of any one particle relative to another is $\frac{4}{3} u_p$. Therefore, the number of collisions per unit volume in unit time τ is

$$N_C = \frac{4}{3} \pi n_p D_p^2 u_p \tau \quad (1)$$

and the rate of collisions

$$\frac{dN_C}{d\tau} = \frac{4}{3} \pi n_p D_p^2 u_p \tau \quad (2)$$

Assumption (1) states that the collision of two particles will result in the formation of a single particle of volume equal to the sum of the volumes of the colliding particles. Therefore, the growth rate of a particle can be expressed as

$$\frac{dv_p}{d\tau} \propto \frac{dN_C}{d\tau} \quad (3)$$

Since a collision of two equal-size particles per unit time would double the particle volume, of three particles triple it, and so forth,

$$\frac{dv_p}{d\tau} = \frac{dN_C}{d\tau} v_p \quad (4)$$

Therefore,

$$\frac{dv_p}{d\tau} = \frac{4}{3} \pi D_p^2 u_p v_p \quad (5)$$

The number of particles per unit volume is expressed as

$$n_p = \frac{v_L}{v_p v_g} \quad (6)$$

Substituting equation (6) into equation (5) yields

$$\frac{dv_p}{d\tau} = \frac{4}{3} \frac{\pi D_p^2 u_p v_L}{v_g} \quad (7)$$

The findings of some investigators of Brownian motion are reviewed in reference 10. The results showed that the total average energy of particles undergoing Brownian motion was equal to the mean kinetic energy of a gas molecule. In the application now under consideration, the particle diameter is less than the mean free path of the surrounding fluid molecules and the particle motion will more closely approach pure molecular motion than Brownian motion. Therefore, the kinetic energy of the particles will be assumed to be equal to the kinetic energy of a gas molecule, and the particle velocity equal to the velocity of an ideal gas molecule of corresponding mass. Reference 10 gives the velocity of an ideal gas molecule as (ref. 10)

$$\xi = \sqrt{\frac{3RT}{M}} \quad (8)$$

Now

$$M = w_p N \quad (9)$$

and

$$w_p = \frac{1}{6} \pi D_p^3 \rho L \quad (10)$$

Therefore,

$$\xi = \sqrt{\frac{18RT}{\pi D_p^3 \rho_p N L}} = u_p \quad (11)$$

Substituting equation (11) into equation (7) gives

$$\frac{dv_p}{d\tau} = \frac{4}{3} \left(\frac{18}{\pi N} \right)^{1/2} \pi \left(\frac{v_L}{v_g} \right) \left(\frac{RT}{\rho_L} \right)^{1/2} (D_p)^{1/2} \quad (12)$$

$$= 12.92 \left(\frac{v_L}{v_g} \right) \left(\frac{RT}{\rho_L} \right)^{1/2} (D_p)^{1/2} \times 10^{-12} \quad (12a)$$

For any set of inlet conditions

$$k' = 12.92 \left(\frac{v_L}{v_g} \right) \left(\frac{RT}{\rho_L} \right)^{1/2} \times 10^{-12} \quad (13)$$

Therefore,

$$\frac{dv_p}{d\tau} = k' (D_p)^{1/2} \quad (14)$$

Since,

$$v_p = \frac{1}{6} \pi D_p^3 \quad (15)$$

then

$$D_p^{1/2} = \left(\frac{6v_p}{\pi} \right)^{1/6} \quad (16)$$

Substituting equation (16) into equation (14) gives

$$v_p^{-1/6} dv_p = k' \left(\frac{6}{\pi} \right)^{1/6} d\tau \quad (17)$$

Setting limits for integration

$$\int_{v_p,0}^{v_p,\tau} v_p^{-1/6} dv_p = k' \left(\frac{6}{\pi} \right)^{1/6} \int_0^\tau d\tau \quad (18)$$

which gives

$$\frac{6}{5} \left(v_{p,\tau}^{5/6} - v_{p,0}^{5/6} \right) = k' \left(\frac{6}{\pi} \right)^{1/6} \tau \quad (19)$$

Substituting $\frac{1}{6} \pi D_p^3$ for v_p yields

$$\left(D_p^{5/2} - D_p^{5/2} \right) = k' \left(\frac{5}{6} \right) \left(\frac{6}{\pi} \right)^{1/6} \left(\frac{6}{\pi} \right)^{5/6} \tau \quad (20)$$

Let

$$k = \left(\frac{5}{6}\right) \left(\frac{6}{\pi}\right)^{1/6} \left(\frac{6}{\pi}\right)^{5/6} k' \quad (21)$$

$$= 1.591 k'$$

The general equation for the growth of a particle is

$$D_{p,\tau}^{5/2} - D_{p,0}^{5/2} = k\tau \quad (22)$$

where

$$k = 20.56 \left(\frac{v_L}{v_g} \right) \left(\frac{RT}{\rho_L} \right)^{1/2} \times 10^{-12} \quad (24)$$

and T is in $^{\circ}\text{K}$, and ρ_L in grams per cubic centimeter.

The simple equation for the particle growth rate obtained is largely due to the initial assumptions. The validity of these assumptions will now be examined for the conditions treated in this investigation. These conditions as previously stated are

Pressure, atm 1 to 1.5
 Temperature, $^{\circ}\text{R}$ 1260 to 2260
 Growth time, millisecond ($\text{sec} \times 10^{-3}$) 2.5 to 30
 Supercooling, $^{\circ}\text{R}$ 1800 to 2200

The assumptions subject to most question are numbers (1), the collision of two or more liquid particles will result in the formation of a single larger particle; and (4), a mean diameter may be assigned and will be typical of the particle diameters at any combustor station.

In regard to assumption (1), reference 7 states that 100-percent collision effectiveness may be expected. The experimental data of reference 8 also verify assumption (1). The change in particle size due to evaporation caused by the surface energy released upon a collision is discussed in a following section.

In regard to assumption (4) the particle distribution curves of reference 9 show that in the aging of smokes not more than a 7-percent deviation from the average particle diameter can be expected in turbulent air for any given set of conditions if all particles have the same terminal diameter. This process is very similar to the one under consideration here. Also, in the nozzles of supersonic and hypersonic wind tunnels, observations of condensation of air and water vapor have been made and a very narrow range of particle diameters at any one station observed; however, there are no published data giving exact values of particle diameters. These observations along with the experimental data of this report (given in a later section) tend to validate this assumption.

Particles Having Brownian Motion and Large Surface Energy

When a liquid surface is in contact with a gas, a force known as surface tension σ is required to maintain the liquid molecules at the liquid surface. The total energy E required to maintain this force for a given surface area A is equal to σA .

The surface energy of 1 gram of n'_p liquid drops with surface tension σ and uniform diameter D_p is

$$E = \sigma A_p n'_p \quad (24)$$

Since

$$n'_p = \frac{6}{\pi D_p^3 \rho}$$

and

$$A_p = \pi D_p^2$$

$$E = \frac{6\sigma}{\rho D_p} \quad (25)$$

This quantity E is large for particle diameters approaching the molecular diameter, and equals the latent heat of vaporization λ (1108 cal/g or 1994 Btu/lb for boric oxide at the normal boiling point) for single molecule particles.

Figure 1 shows the percentage of the latent heat of vaporization contained in the surface energy of a given weight of liquid boric oxide particles of constant diameter (calculated from eq. (25)).

When two particles a and b collide and form a new particle c , the surface energy released is

$$(E_a + E_b) - E_c = \Delta E \quad (26)$$

$$\sigma A_a + \sigma A_b - \sigma A_c = \Delta E \quad (27)$$

For example, if $A_a = A_b$ and since $v_a + v_b = v_c$, $D_c = 2^{1/3} D_a$. Therefore,

$$\Delta E = (2 - 2^{2/3}) A_a \sigma \quad (28)$$

The fraction of the initial surface energy released upon the collision of two particles of equal diameter is

$$\frac{\Delta E}{2E_a} = \frac{(2 - 2^{2/3})}{2} = 0.206 \quad (29)$$

The quantity of heat given up upon a collision of two particles as a function of particle diameter is shown in figure 2. This energy unless rejected to the surroundings will raise the temperature of the particle. If the temperature is raised above the saturation temperature, evaporation will reduce the size of the combined particle. (See CONCLUDING REMARKS.)

Assume 1 pound of liquid boric oxide particles, each 5×10^{-7} centimeter in diameter. If each particle collides with another particle, the heat released is calculated as follows:

From figure 1, 18 percent of λ is held by surface forces. Therefore, the heat release is

$$0.18 \times 1994 \times 0.206 = 72 \text{ Btu}$$

and the temperature rise is

$$\frac{72}{0.213} = 339^{\circ} \text{ R}$$

($c_p = 0.213 \text{ Btu}/(^{\circ}\text{F})(\text{lb})$ or $\text{cal}/(^{\circ}\text{C})(\text{g})$ from ref. 2).

The rate at which this energy will be dissipated to the surroundings will be proportional to the number of collisions the particle makes with gas molecules before it collides with another liquid particle and releases more energy. For a pentaborane equivalence ratio of 0.20 at 1 atmosphere pressure and a particle diameter of 5×10^{-6} centimeter, the time between liquid particle collisions from equation (22) is 1.62×10^{-11} second. The number of collisions the original particle makes with gas molecules before colliding with another liquid particle is 2.9×10^2 . If it is assumed that each colliding molecule comes to temperature equilibrium with the liquid particle, this number of collisions is sufficient to reduce the temperature of the liquid particle enough so that negligible evaporation would occur. Calculations of the foregoing type indicate that where the degree of supercooling is at least 700° R it is unnecessary to consider surface energy at all and equation (22) may be used to express the particle growth rate in the region. If the supercooling is less than 700° R , it is possible that no condensation will occur; and in any event, a stepwise solution of equation (22) in conjunction with the result of equation (29) must be used to obtain particle growth rates.

From this method of calculating stepwise particle growth, the time required for a particle to grow to a diameter of 2.2×10^{-6} centimeter is less than 1×10^{-6} second for 1800° R supercooling. The value of 2.2×10^{-6} centimeter is the minimum diameter where surface energy may be neglected as calculated by the method of reference 11. Growth times of the order of 1×10^{-6} second are of interest in the expansion of boron-fuel combustion products through a nozzle at high combustion temperatures (above 3840° R unless the combustion pressure is greater than 1.5 atm, at which point temperatures as low as 3460° R should be considered). Therefore, for the conditions under study in this report (maximum temperature, 2260° R) the time required for growth to a diameter of 2.2×10^{-6} centimeter will be neglected.

In reference 11 an analysis of the condensation of water vapor is presented. The time required for the liquid water particles to grow to a diameter where surface forces are negligible (for water, $1 \times 10^{-7} \text{ cm}$) is calculated to be less than 1×10^{-6} second, which is similar to the value calculated for boric oxide.

The preceding analysis assumed spherical particles, which is not the case if only a small number of molecules make up a single particle. However, the effect of particles of this type is considered small because of their short life and will be neglected.

Particles Having Negligible Surface Energy

In the diameter range where surface energy may be neglected ($D_p > 2.2 \times 10^{-7}$ cm), equation (22) may be used to describe the particle growth directly.

EXPERIMENTAL APPARATUS AND PROCEDURE

General

The experimental work was performed in a 4-inch connected-pipe facility supplied with metered combustion air from the laboratory central air system (fig. 3). A perforated plate (fig. 4) blocked 70 percent of the pipe area 1/4 inch upstream of the plane of fuel injection. A high pressure drop ($\Delta p/p = 0.27$ at an inlet-air velocity of 175 ft/sec) across the perforated plate served to achieve rapid mixing in the combustion zone and a flat temperature and velocity profile. Fuel was injected normal to the air flow from three points in each of six arms extending through holes in the perforated plate (see figs. 4 and 5). Ignition was supplied by means of a spark plug 8 inches downstream of the perforated plate.

The 18-inch-long section of pipe immediately downstream of the perforated plate was replaced with a Lucite tube (4-in. I.D. by $4\frac{1}{2}$ -in. O.D.) for three preliminary tests. The purpose of these tests was to determine temperature and velocity profiles and to observe visually and photographically the pentaborane flame. Motion pictures of the flame were taken through the Lucite at a camera speed of 128 frames per second and a lens setting of f/11.

The fuel system (fig. 6) was designed for use with boron hydrides and provided for remote operation, flushing, and cleaning of fuel lines and injector. After each run, the injector was immediately flushed out with helium to prevent decomposition of the pentaborane fuel. The lines were then flushed with JP-4 fuel to remove excess pentaborane, which was followed by a 50 percent methanol - 50 percent acetone mixture that reacted with any remaining pentaborane to form nontoxic noncombustible products. Finally the lines were again flushed with JP-4 fuel to remove all traces of fuel or fuel residue. Fuel flow was measured with a rotating-vane-type flowmeter and recorded on a self-balancing strip-chart recorder.

Temperature, static pressure, and total pressure were measured and recorded at three equidistant stations between the perforated plate and the sampling probe. These measurements were used to determine combustion efficiencies and temperature and velocity profiles. Combustion efficiencies were computed by the method of reference 12.

Particle Sampling Probe and Quench Technique

A probe for collecting and freezing the liquid boric oxide combustion product was placed at one of three distances downstream of the perforated plate: 36.5 inches, 53 inches, or 128.5 inches. The probe detail is shown in figure 7. Liquid nitrogen was supplied from a 100-liter Dewar flask under helium pressure and injected through the inner wall of the probe at a point 3 inches from the probe inlet. Gaseous nitrogen was also injected at this point and atomized the liquid nitrogen. The quantity of liquid nitrogen injected was not measured, but was sufficient to drop the temperature of the collected stream to $250^{\circ}\pm 50^{\circ}$ F. At this temperature the boric oxide in the exhaust stream is a solid and the other components gaseous. Temperature measurements showed that the quenching of the collected stream was virtually complete in a maximum distance of 3 inches after injection of liquid nitrogen.

Particle Collection System

A 2-inch-diameter rubber hose carried the collected stream from the sampling probe to the particle collector. An electronic particle precipitator (see fig. 3) was used to remove the solid particles from the gas stream. According to the manufacturer's specifications the collection efficiency of the particle precipitator is 87 percent for particles 1×10^{-5} centimeter in diameter, and 99 percent for particles 9×10^{-5} centimeter in diameter.

The collection medium was 1/16-inch Fiberglas matting, and was replaced after each run. Figure 8 shows the appearance of the Fiberglas mat with its mounting frame after a typical run. The collected stream with solid particles removed was then returned to the main combustion gas stream. A butterfly valve located in the return line was used to control the stream velocity entering the probe.

General Description of Typical Test

Before each test the filter was loaded with new collection media, the fuel-system pressure checked and flushed with helium, and the liquid nitrogen lines hooked up. After air flow and inlet-air temperature were

established, the liquid-nitrogen flask was pressurized and 3 minutes allowed for the liquid nitrogen lines to cool. The fuel bottle was pressurized and the fuel throttle set to give the desired fuel-air ratio. The fuel was turned on and once a flame was established (as evidenced by total pressure and temperature rise) 5 seconds were allowed for instruments to come to equilibrium. The instrument recorders were then turned on and after 12 seconds (one instrument cycle) the fuel was turned off and the lines purged as described earlier.

Particle Analysis

The Fiberglas mat was removed from the particle precipitator and a small portion washed with n-heptane (C_5H_{12}) to remove the boric oxide particles. Boric oxide is insoluble in n-heptane. A portion of the resulting suspension of boric oxide particles in n-heptane was deposited on electron microscope grids. The n-heptane was evaporated, leaving the boric oxide particles. A minimum of three electron-photomicrographs was taken of samples from each run. Examples of the electron-photomicrographs are shown in figure 9. The magnification of the electron microscope was calibrated and the size of each particle in the photographs measured. Approximately 50 particles were measured for each run. From these measurements an average particle diameter was determined by plotting observed diameter against percentage of total number of particles having that diameter (see fig. 10). The particle agglomerates shown were formed in the particle precipitator and the heptane suspension. Careful visual observation of the agglomerates under the electron microscope showed they were made up of a number of smaller particles of approximately spherical shape, some of which are outlined in figure 11. Fifty measurements were considered sufficient for the analysis because of the very narrow range of sizes encountered. The probable error in average particle diameter was calculated to be ± 1.4 percent for run 6, which gave the largest spread of measured particle diameters. The error in actual measurement of the particle diameters was within ± 3 percent.

Calculation of Liquid Particle Residence Time

The flame length was determined by temperature measurements and photography. It was assumed that the pentaborane enters the combustor as a vaporizing liquid droplet surrounded by air and burns near the stoichiometric flame temperature. The boric oxide thus formed is in the vapor state and is later condensed by the rapid mixing with additional air. The point where the condensation of the boric oxide occurs

was assumed to coincide with the point where the flame becomes non-luminous. With these assumptions the time available for particle growth τ can be expressed by

$$\tau = \frac{l_T - l_F}{u_s} \quad (30)$$

where l_T is the distance from the perforated plate to the liquid nitrogen quench station; l_F is the photographically determined flame length; and u_s is the mean stream velocity. In some tests, the photographically determined flame length was compared with the values indicated by thermocouple measurements.

Range of Experimental Program

The experimental program covered a pentaborane equivalence-ratio (actual fuel-air ratio divided by stoichiometric fuel-air ratio) range of 0.074 to 0.22 and a combustor static-pressure range of 1 to 1.4 atmospheres. The inlet-air temperature was held constant at 580° R and the inlet-air velocity varied from 130 to 250 feet per second. The total time available for particle growth varied from 2.5 to 30 milliseconds.

RESULTS

Comparison of Flame Lengths Determined from Photographs and from Thermocouples

From the photographic studies made with the replaceable Lucite tube, a flame length of 16 to 18 inches was observed over an equivalence-ratio range of 0.10 to 0.24. The use of visible flame length as a criterion for determining the length of the combustion zone was partially confirmed by making thermocouple measurements during representative runs. For example, in preliminary test 2 the temperature was 1800° F 22 inches downstream of the fuel injector while a thermocouple 16 inches downstream of the fuel injector was burned off, which indicates that the combustion reaction had not been completed at that point. A flame length of 18 inches was observed from motion pictures. Therefore, when using equation (35) for determining time available for particle growth, a value of 18 inches was used for l_F . A photograph of the pentaborane flame in the Lucite section is shown in figure 11.

Combustion Efficiency

A combustion efficiency of 100 percent was achieved during each of the tests. Also a chemical analysis of the collected samples showed them to be 100 percent boric oxide.

Temperature and Velocity Profile

Figure 12 shows the temperature and velocity profiles for run 2, which was typical for each of the runs. For any one run the maximum temperature-profile spread from the mean temperature was 5 percent or less, and the maximum velocity profile spread from the mean velocity 10 percent or less at a station 22 inches downstream of the perforated plate. The highest velocity occurred about 1/2 inch from the center and was due to the penetration of the jets through the holes in the perforated plate. These jets decayed very rapidly from this point on, and were not noticeable at a point 30 inches downstream of the fuel injector.

Particle Size and Growth Rate

A summary of the experimental data appears in table I.

Over the entire range of experimental conditions covered, the measured average particle diameters fell between 1.10×10^{-5} and 1.46×10^{-5} centimeter, and the particles were very nearly spherical in shape. The experimentally measured particle diameters are shown plotted against particle diameter calculated from equation (22) for the same conditions and residence time in figure 13. The average deviation of the measured diameter from the calculated diameter was 27 percent, which gives a probable error of ± 34.1 percent. If the sign of the deviation is taken into account (greater or less than theoretical), the arithmetic average deviation is 16.4 percent.

Particle Size in Turbojet Combustor

The perforated-plate-type combustor and connected pipe used in the experimental work very closely approximate a ram-jet-type combustor; therefore, the experimental results are very easily applied to ram-jet calculations. To verify the experimental results for use on turbojet applications, a single run was made with the sampling probe at the outlet of the J47 tubular combustor reported in reference 6. Pentaborane fuel was burned at an equivalence ratio of 0.176. The reference velocity was 103 feet per second and the inlet-air temperature 580° R. The boron oxide particle size was 1.23×10^{-5} centimeter. This diameter

corresponds to a residence time of about 7 milliseconds. The exact residence time in a tubular combustor is unknown, but 7 milliseconds is a reasonable value.

DISCUSSION AND APPLICATION OF RESULTS

General

It appears from both the theoretical and experimental data that the liquid boric oxide particles found in the combustion products of a jet engine burning a boron-containing fuel grow very rapidly to a diameter of about 1.0×10^{-5} centimeter. In the normal jet-engine residence time, the particles would never exceed a diameter of about 2.0×10^{-5} centimeter unless allowed to contact a surface where larger particles would be torn from the resultant film. This is illustrated in figures 14 and 15.

The experimental data do not constitute an extremely critical test of the theory. The rather narrow range of particle diameters encountered probably accounts for the good data correlation obtained. Difficulties encountered in making accurate particle-size measurements probably account for some of the deviation of the experimental results from the theory. However, equation (22) will give agreement within ± 45 percent with the experimental results when calculating liquid boric oxide particle diameters.

The very narrow range of particle sizes encountered might indicate that condensation occurred in the collection probe. However, it was felt that this was not the case for the following reasons:

- (1) 100 Percent combustion efficiency was measured from the temperature rise across the combustor. Because of the high heat of vaporization of boric oxide, the temperature rise would have been about 18 percent less if the boric oxide had not been in the liquid state.
- (2) The degree of supercooling was sufficient for rapid condensation to occur immediately downstream of the flame zone.
- (3) The very short time available for particle growth allowed after injection of the liquid nitrogen (before fusion occurred) would make it very unlikely that the particles would grow to the diameters encountered.

It is fortunate, from the standpoint of over-all engine efficiency, that the particle diameters are in the size range of 1×10^{-5} to 1.5×10^{-5} centimeter. These particle diameters are large enough so that the surface energy is only about 1 percent or less of the latent heat of vaporization and yet small enough that the drag coefficients and heat-transfer coefficients based on the particle diameter are essentially infinite.

Performance Calculations

By using equation (22), a boric oxide particle diameter may be calculated for conditions in the range of interest. This equation is expressed in general terms, and may be used regardless of the fuel used (boron-hydrogen or boron-carbon-hydrogen). This will make analytical evaluations of drag forces acting on the particle and heat-transfer rates to and from the particles (ref. 1) possible. These calculations, in turn, will make more accurate analytical determinations of performance parameters attainable for all boron-containing fuels.

Oxide Deposition on Engine Surfaces

From the experimentally determined particle diameters it appears likely that most of the boric oxide found on engine surfaces is deposited by particle diffusion, or at least may be treated as a diffusional process. The rate of diffusion of a substance to a surface may be expressed, in general, by Fick's law (ref. 13)

$$\frac{m}{A} = K \frac{dc}{dl} \quad (31)$$

where K is a function of the type of diffusion occurring (turbulent or molecular).

Integration of equation (31) from 0 to l and from C_s to C_w gives

$$m = K \frac{(C_s - C_w)}{l} A \quad (32)$$

Assume that all particles coming in contact with a wall remain on the wall, as would be the case with viscous liquid droplets. Therefore, the concentration of particles in the gas adjacent to the wall will approach zero. Equation (32) becomes

$$m = K \frac{C_s - 0}{l} A = K \frac{C_s A}{l} \quad (33)$$

The particle concentration in the main gas stream C_s is finite and essentially constant across any flow-channel cross section. A steep concentration gradient must then exist across a thin gas film adjacent to the wall, which is the diffusion boundary layer.

The flow pattern of gases in a jet-engine combustor is extremely complex and not well enough defined to permit a calculation of the diffusion boundary-layer thickness δ . Also, the diffusion mechanism is

not defined, and, consequently, K is unknown. The simplest method of accurately determining δ and K would be experimentally on carefully controlled surfaces in a combustor. Once δ and K are known, deposition rates on engine surfaces may be calculated from equation (33) by substituting δ for l and the correct value of K .

In view of the small particle sizes, it is now possible to suggest some methods that might eliminate or at least reduce engine deposits.

It is seen from equation (33) that the rate of deposition on a surface will be inversely proportional to δ . Increasing δ several times would decrease the deposition rate by a like amount. This increase in diffusion boundary-layer thickness may be accomplished by several methods: (1) introducing an air film along the surface on which deposition is occurring; (2) cooling this air film to freeze the particles before they hit the wall so that they might be easily swept off; or (3) introducing a mechanical device that would induce boundary-layer growth.

The effect of a cold-air film on deposition rates is illustrated when the conventional combustor-liner deposition rates of references 14 and 15 are compared with the deposition rate on the experimental wire-cloth combustor liner of reference 16. This comparison is shown in figure 16. The wire cloth allowed a continuous flow of secondary combustion air which filmed the liner surface, reducing boric oxide deposits 100 times.

For particles formed by the growth process discussed herein, there is little possibility of any particle in the gas stream being large enough to contact a surface because of its own inertia. This could conceivably occur, however, if particles of larger size were formed by some other means. One probable source of larger particles is as follows: With improper fuel-injector design some fuel is sprayed directly onto the walls of the combustor. This results in films of molten boric oxide (which might also be deposited by diffusion) on the walls. As these films flow past sharp corners or air-entry ports, large particles are torn from the film. To eliminate particles of this type, care must be taken in the design of engine components to eliminate surfaces that might generate films of molten boric oxide.

CONCLUDING REMARKS

The calculations which resulted in figures 1 and 2 were based on the assumptions that the surface tension of the infinite liquid is valid when applied to small liquid particles made up of a very few molecules, and that these particles are spherical in shape. Both of these assumptions are difficult to justify, but were made for lack of anything better. Consequently, the error involved in using figures 1 and 2 is probably large. However, these figures indicate a trend and are probably within an order of magnitude of the actual values.

Lewis Flight Propulsion Laboratory

National Advisory Committee for Aeronautics
Cleveland, Ohio, September 26, 1955

APPENDIX - METHOD OF CALCULATING v_L/v_g FOR ANY

FUEL CONTAINING BORON, CARBON, AND HYDROGEN

AT COMBUSTION TEMPERATURES BELOW 2500° F

Calculation of v_L/v_g

With 1 pound of inlet air as a basis, the total weight of oxygen used by a combustion reaction at the stoichiometric fuel-air ratio (f/a)* is 0.2329 pound. An oxygen balance for the combustion of a fuel containing boron, carbon, and hydrogen gives the following equation:

$$0.2329 = \left[\frac{x_B(f/a)^*}{M_B} \right] \times \frac{3}{4} \times 32.00 + \left[\frac{x_C(f/a)^*}{M_C} \right] \times 32.00 + \left[\frac{x_{H_2}(f/a)^*}{M_{H_2}} \right] \times \frac{1}{2} \times 32.00 \quad (A1)$$

Substituting the correct values for M_B , M_C , and M_{H_2} (the molecular weights of boron, carbon, and hydrogen, respectively) and solving for $(f/a)^*$ gives

$$\left(\frac{f}{a} \right)^* = \frac{1}{9.552 x_B + 11.44 x_C + 34.07 x_{H_2}} \quad (A2)$$

which gives the stoichiometric fuel-air ratio as a function of the weight fraction of boron, carbon, and hydrogen in the fuel (x_B , x_C , and x_{H_2}).

Equivalence ratio ϕ is defined as

$$\phi = \frac{(f/a)_{actual}}{(f/a)^*} \quad (A3)$$

The total molar flow of exhaust gases per pound of inlet air $n_{m,T}$ (assuming all the boron oxide is in the liquid state and will be neglected) may be expressed by

$$n_{m,T} = 0.02737 + 0.02272 \left(\frac{f}{a} \right) (x_C) + 0.0550 \left(\frac{f}{a} \right) (x_{H_2}) + (1 - \phi) (0.007278) \quad (A4)$$

If the combustion temperature T_c and combustion static pressure p_c are known, the volumetric flow of the exhaust gases v_g per pound of inlet air can be calculated, using

$$v_g = \frac{0.730 n_m, T_c}{p_c} \quad (A5)$$

The volume of liquid in the exhaust gases v_L per pound of inlet air is calculated from

$$v_L = 3.218 \left(\frac{f}{a} \right) \left(\frac{x_B}{\rho_L} \right) \quad (A6)$$

The value of ρ_L (density of boric oxide, glass) is taken from figure 17.

From equations (A5) and (A6), the volume concentration of boron oxide v_L/v_g is easily calculated for any boron-carbon-hydrogen fuel.

REFERENCES

1. Barry, F. W.: Performance of a Ramjet Burning Pentaborane - Effect of Liquid Droplets in Exhaust Nozzle. Rep. AL-1712, Missile and Control Equip., North Am. Aviation, Inc., Oct. 28, 1953.
2. Rossini, Frederick D., et al.: Selected Values of Chemical Thermodynamic Properties. Cir. 500, NBS, Feb. 1952.
3. Thomas, C. A., and Eads, E. K.: Boric Oxide Deposition. Rep. CCC-1024-TR-15, Callery Chem. Co., Mar. 31, 1954.
4. Smoluchowski, M. V.: Versuch einer mathematischen Theorie der Koagulationskinetik kolloider Lösungen. Zs. Phys. Chem., Bd. 92, Heft 2, 1917, pp. 129-168.
5. Speiser, Rudolph, Naiditch, Sam, and Johnston, Herrick L.: The Vapor Pressure of Inorganic Substances. II. B₂O₃. Jour. Am. Chem. Soc., vol. 72, no. 6, June 14, 1950, pp. 2578-2580.
6. Branstetter, J. Robert, and Kaufman, Warner B.: Altitude Performance of Pentaborane - JP-4 Fuel Blends in a Modified J47 Combustor. NACA RM E54H16, 1957.
7. Anon.: Handbook on Aerosols. United States Atomic Energy Comm., 1950.
8. Whytlaw-Gray, R. W., and Patterson, H. S.: Smoke. Edward Arnold & Co. (London), 1932.

9. Langstroth, G. O., and Gillespie, T.: Coagulation and Surface Losses in Disperse Systems in Still and Turbulent Air. Canadian Jour. Res., vol. 25, sec. B, 1947, pp. 455-471.
10. Loeb, Leonard B.: The Kinetic Theory of Gases. Second ed., McGraw-Hill Book Co., Inc., 1934.
11. Rodebush, W. H.: Nuclei in Evaporation and Condensation. Chem. Rev., vol. 44, no. 2, Apr. 1949, pp. 269-276.
12. Huff, Vearl N., Gordon, Sanford, and Morrell, Virginia E.: General Method and Thermodynamic Tables for Computation of Equilibrium Composition and Temperature of Chemical Reactions. NACA Rep. 1037, 1951. (Supersedes NACA TN's 2113 and 2161.)
13. Kruyt, H. R., ed.: Colloid Science. Vol. I. Elsevier Pub. Co., 1952.
14. Gibbs, J. B., Kaufman, W. B., and Branstetter, J. R.: Preliminary Investigation of the Combustion of Pentaborane and Diborane in a Turbojet Combustor at Simulated Altitude Conditions. NACA RM E53B18, 1957.
15. Branstetter, J. Robert, Kaufman, Warner B., and Gibbs, James B.: Preliminary Investigation of the Combustion of a 50 Percent Pentaborane - 50 Percent JP-4 Fuel Blend in a Turbojet Combustor at Simulated Altitude Conditions. NACA RM E53J21, 1957.
16. Kaufman, Warner B., and Branstetter, J. Robert: Preliminary Investigation of the Altitude Performance of Pentaborane and a Pentaborane - JP-4 Blend in an Experimental 9.5-Inch-Diameter Tubular Combustor. NACA RM E53J19, 1957.
17. Einstein, A.: Zur Theorie der Brownschen Bewegung. Ann. Phys., Bd. 19, 1906, pp. 371-381.
18. Smoluchowski, M. V.: Zur kinetischen Theorie der Brownschen Molekularbewegung und der Suspensionen. Ann. Phys., Bd. 21, Heft 14, 1906, pp. 756-780.
19. Perry, John H., ed.: Chemical Engineers' Handbook. Third ed., McGraw-Hill Book Co., Inc., 1950.
20. Hodgman, Charles D., ed.: Handbook of Chemistry and Physics. Thirty-second ed., Chem. Rubber Pub. Co., 1950-1951.

TABLE I. - EXPERIMENTAL DATA BASED ON 1 GRAM OF INLET AIR PER SECOND

Run	Fuel flow, g/sec	Inlet-air reference velocity, ft/sec	Equiv-alence ratio, ϕ	Combustion temperature, T , $^{\circ}$ R	Combustion pressure, p , atm	Weight flow of boric oxide, g/sec	Volume flow of boric oxide, v_L , cc/sec
1	0.01305	134	0.1708	1950	1.046	3.602×10^{-2}	2.345×10^{-2}
2	.01561	142	.2043	2188	1.026	4.308	2.837
3	.008389	250	.1098	1495	1.042	2.315	1.476
4	.007938	132	.1039	1448	1.058	2.191	1.393
5	.005661	183	.0741	1200	1.233	1.562	.9842
6	.008198	200	.1073	1478	1.303	2.263	1.441
7	.01065	175	.1349	1721	1.419	2.939	1.892
8	.01075	179	.1407	1732	1.416	2.967	1.911
9	.01040	161	.1361	1700	1.169	2.870	1.846
10	.01233	188	.1614	1881	1.188	3.403	2.208
11	.009947	184	.1302	1655	1.128	2.745	1.761
12	.01683	160	.2203	2299	1.138	4.645	3.076

Run	Particle diameter calculated from equation (22)	Total growth time, τ , sec	Final particle diameter, D_p, τ , cm	Combustor exit velocity, u_s , ft/sec	Boric oxide volume concentration, v_L/v_g , cc/cc	Experi-mental D_p	Distance from perforated plate to quench station, in.
						Calcu-lated D_p	
1	1.025×10^{-5}	6.373×10^{-3}	1.17×10^{-5}	458	9.650×10^{-6}	1.141	53
2	1.005	5.384	1.37	541	10.23	1.363	
3	.842	5.763	1.20	506	7.704	1.425	
4	1.620	30.12	1.32	306	7.567	.815	128.5
5	1.480	24.57	1.46	375	7.130	.986	
6	1.223	21.09	1.42	436	9.518	1.161	
7	1.800	22.71	1.15	405	11.91	.639	
8	1.741	20.54	1.10	448	11.93	.632	
9	1.528	19.06	1.25	483	9.516	.821	
10	1.522	16.00	1.35	576	10.63	.887	
11	1.458	17.94	1.16	513	9.054	.796	
12	.790	2.493	1.37	619	11.75	1.730	36.5

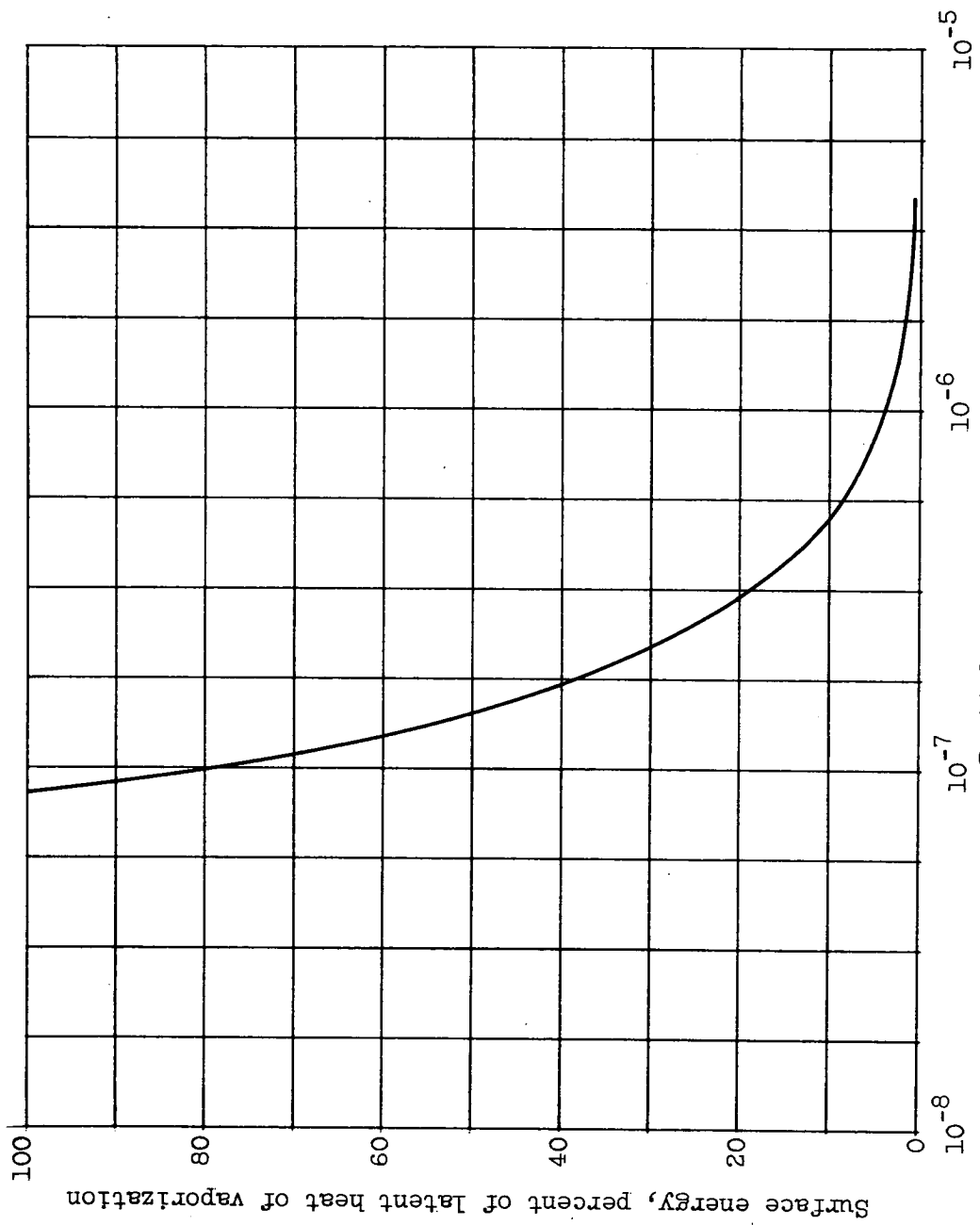


Figure 1. - Surface energy of small boric oxide particles. Temperature, 1980° R.

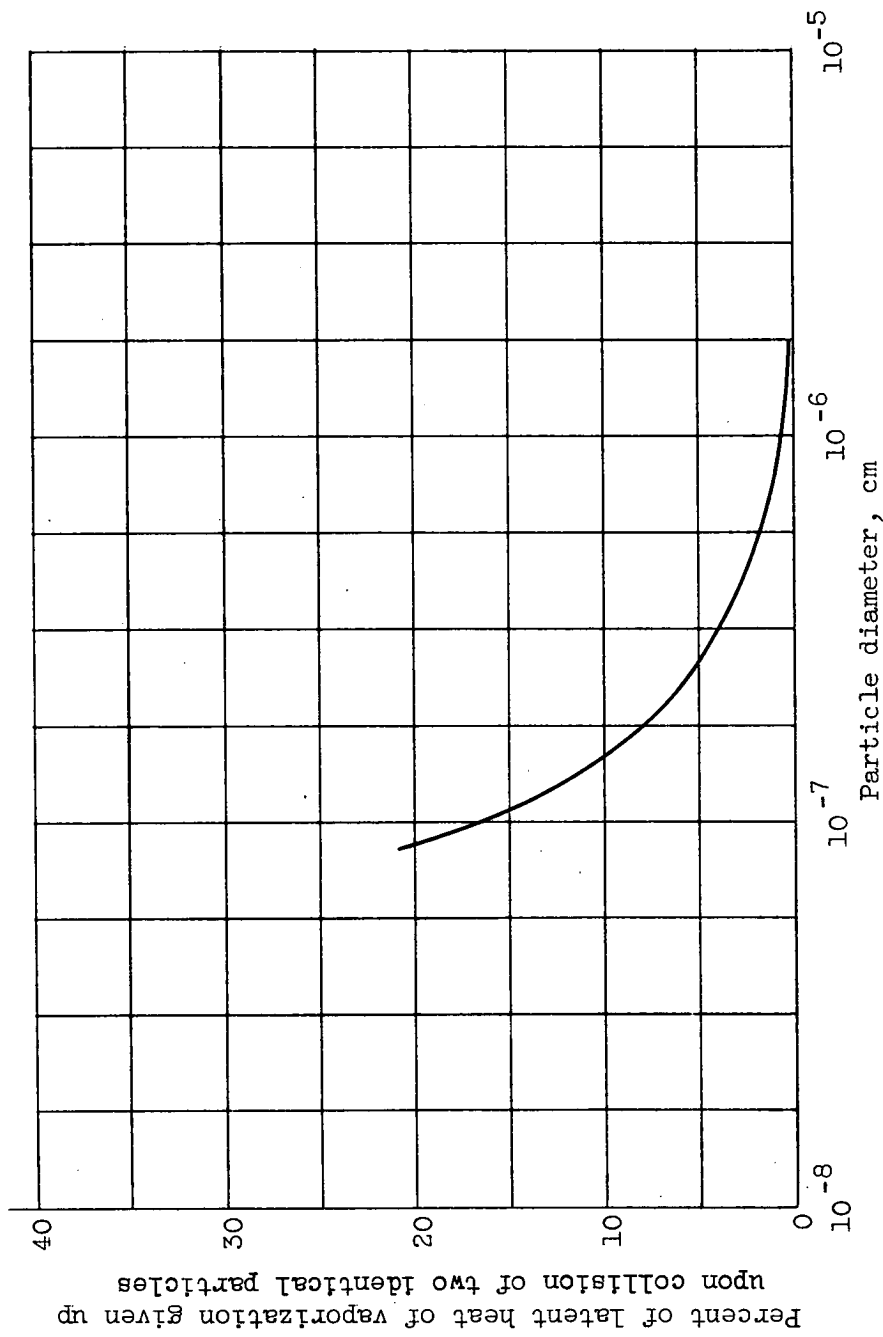


Figure 2. - Percent of latent heat of vaporization evolved upon collision of two identical particles. Temperature, 1980° R.

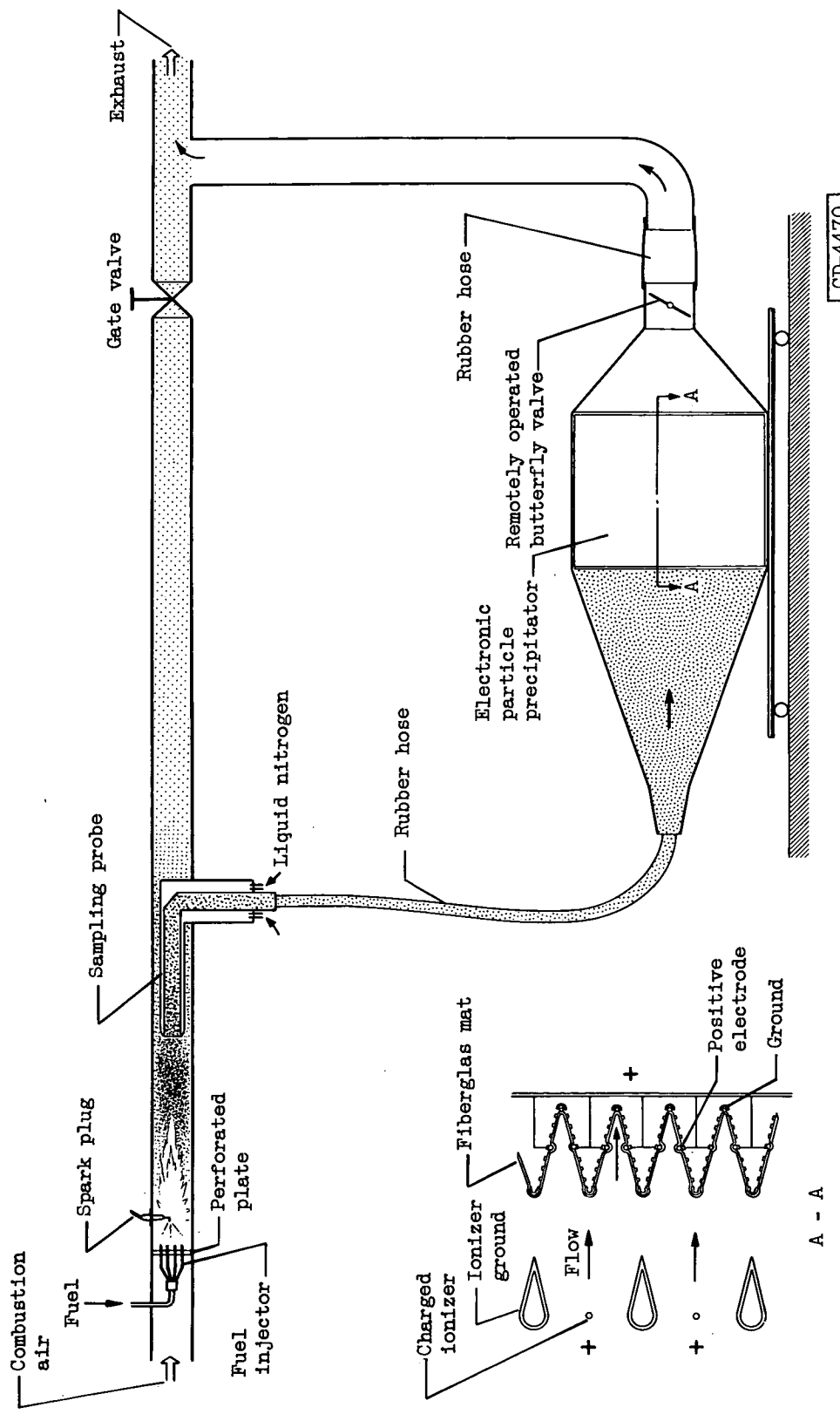


Figure 3. - Schematic diagram of experimental apparatus.

C-37536

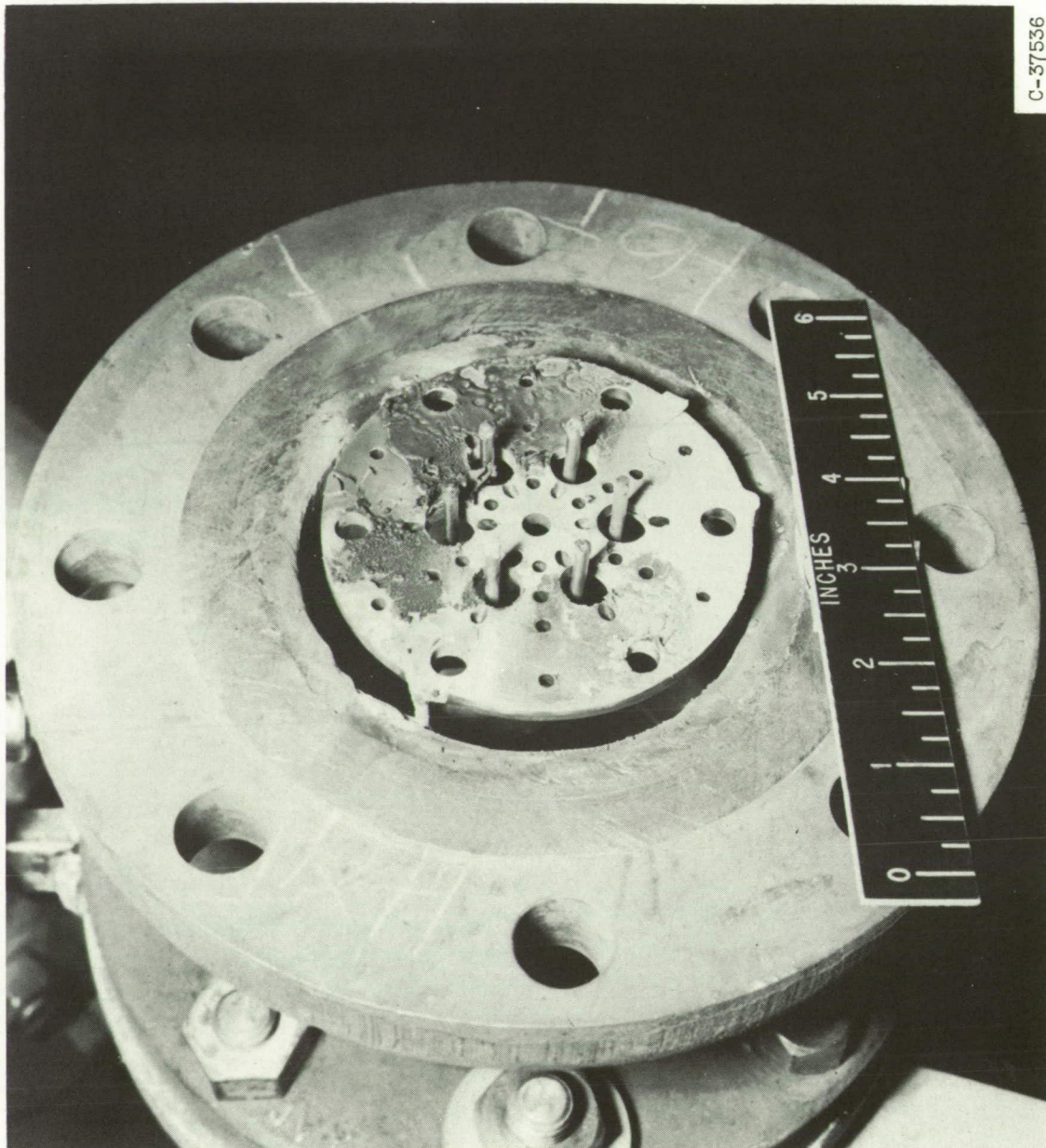
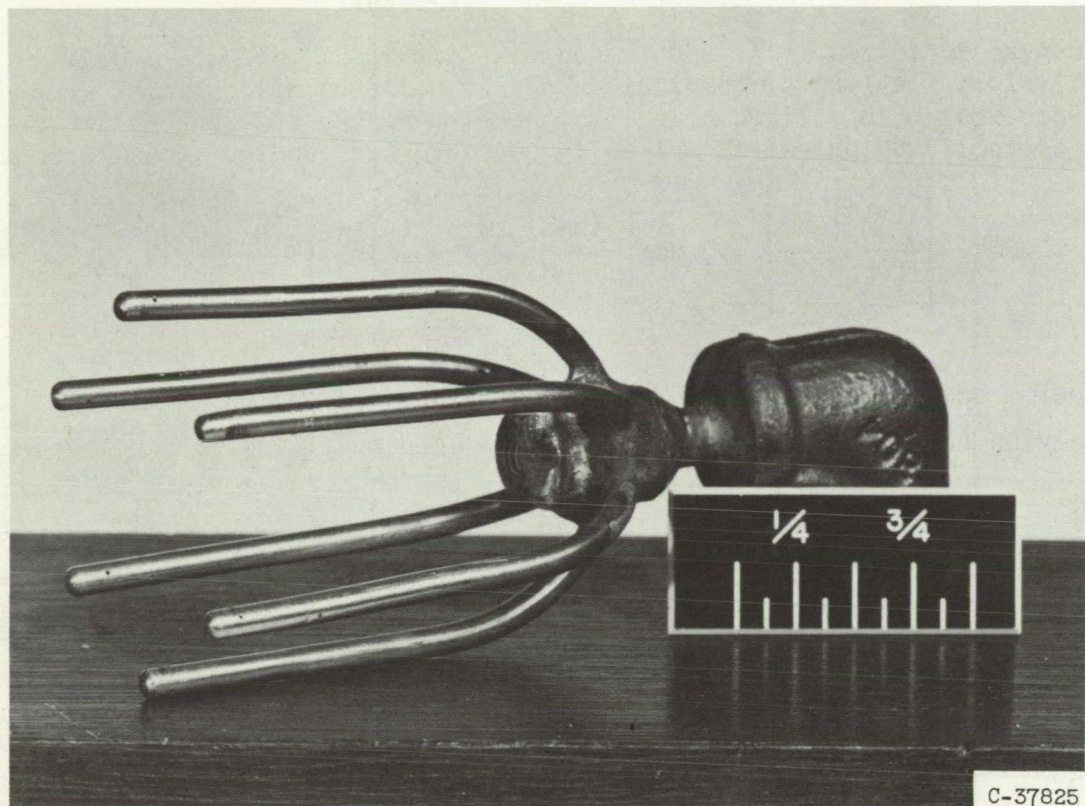


Figure 4. - Perforated plate and fuel injector after 70 seconds of operation (preliminary run 2).



C-37825

Figure 5. - Fuel injector.

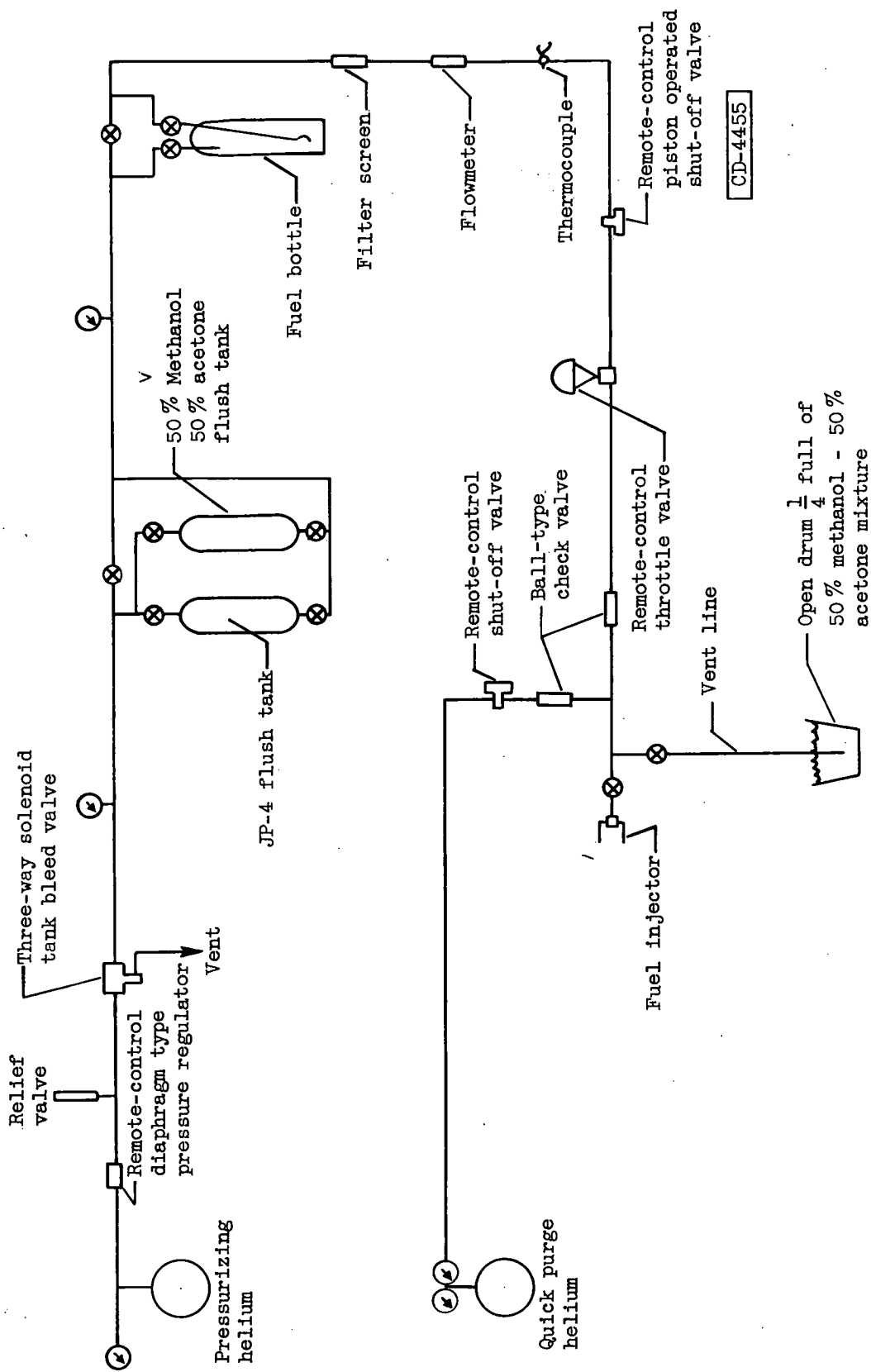


Figure 6. - Schematic diagram of fuel system.

- A Liquid nitrogen for injection
- B Liquid nitrogen for cooling
- C Gaseous nitrogen for atomization
- D Inner wall static-pressure tap
- E Outer wall static-pressure tap

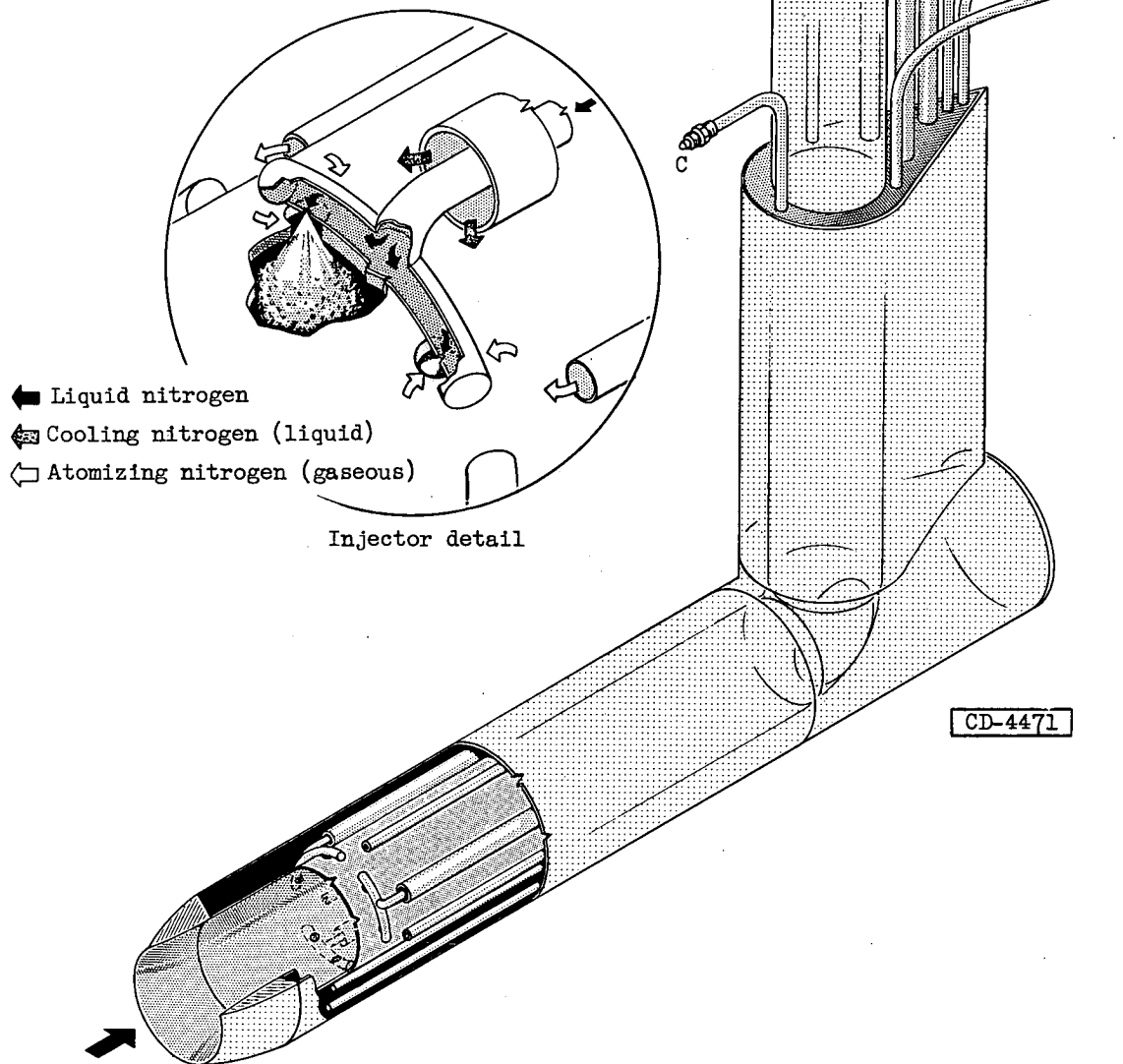


Figure 7. - Detail of sampling probe.

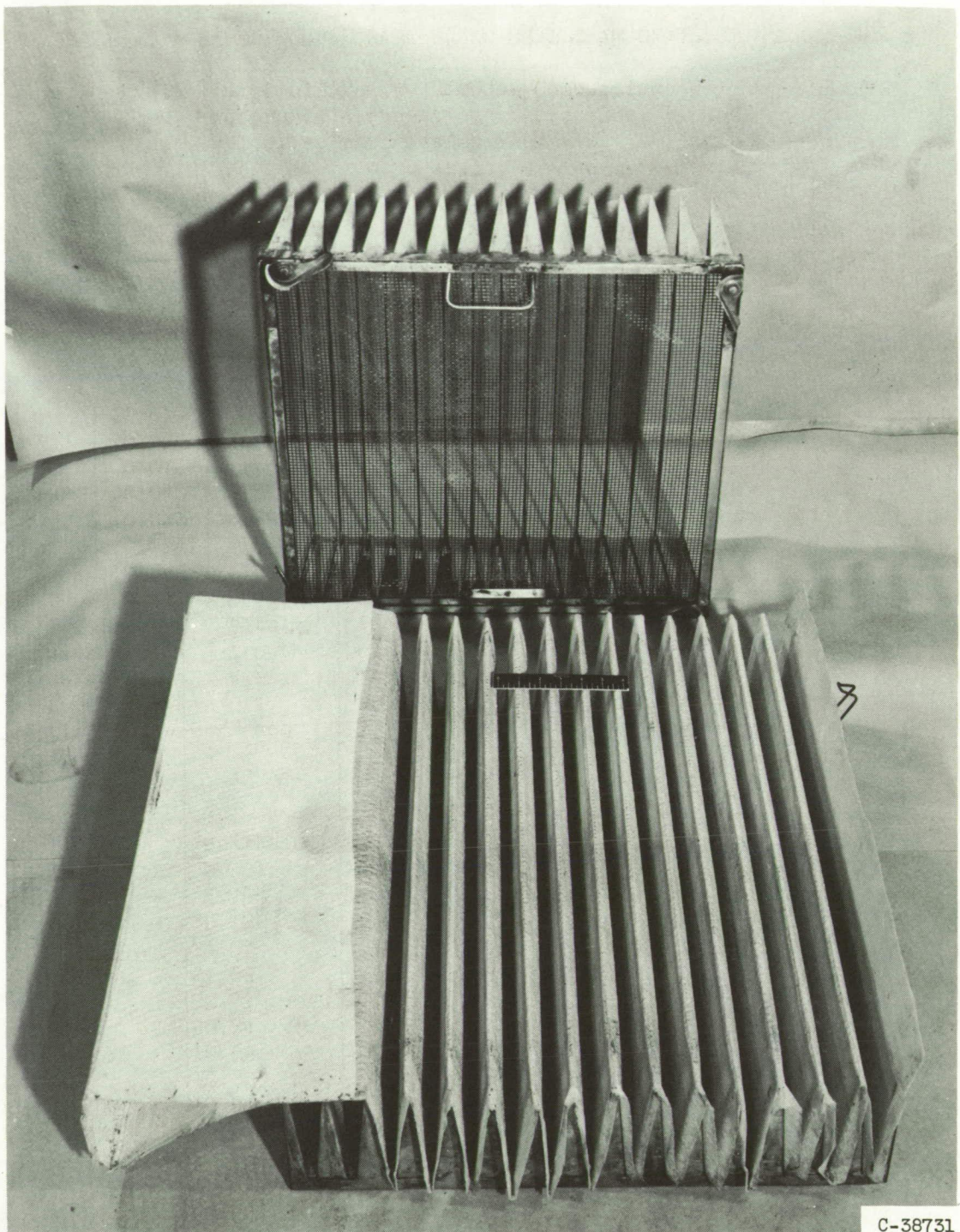
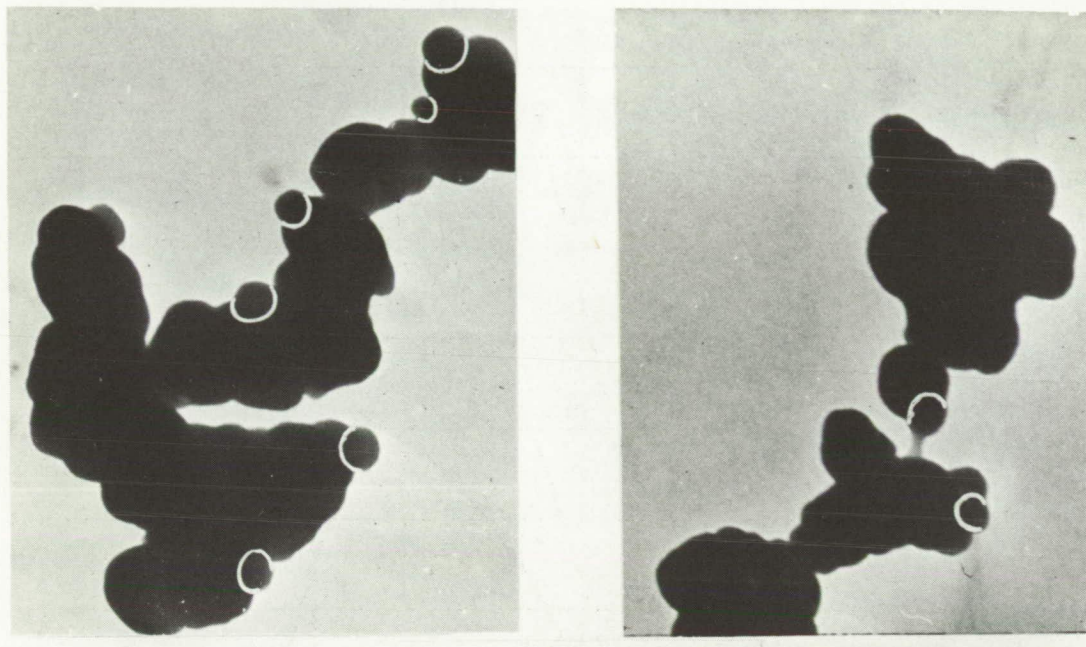
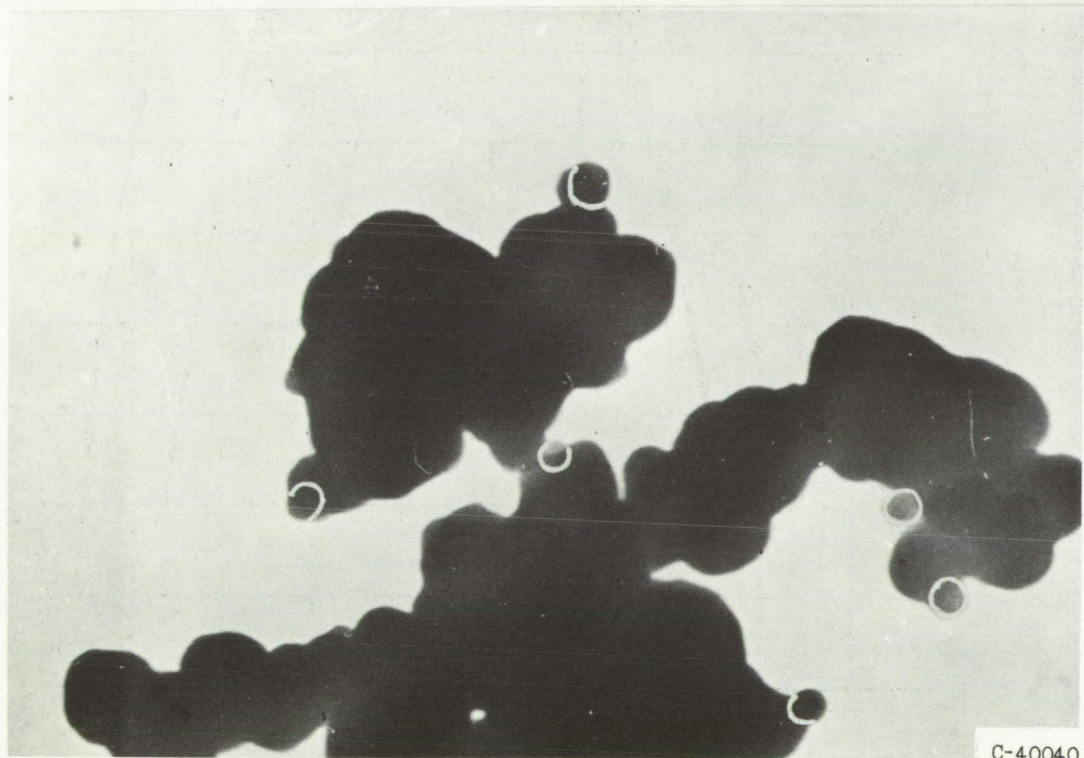


Figure 8. - Fiberglas collection media after typical run (run 9).



0 0.5 1.0
μ



C-40040

Figure 9. - Typical boric oxide particles.

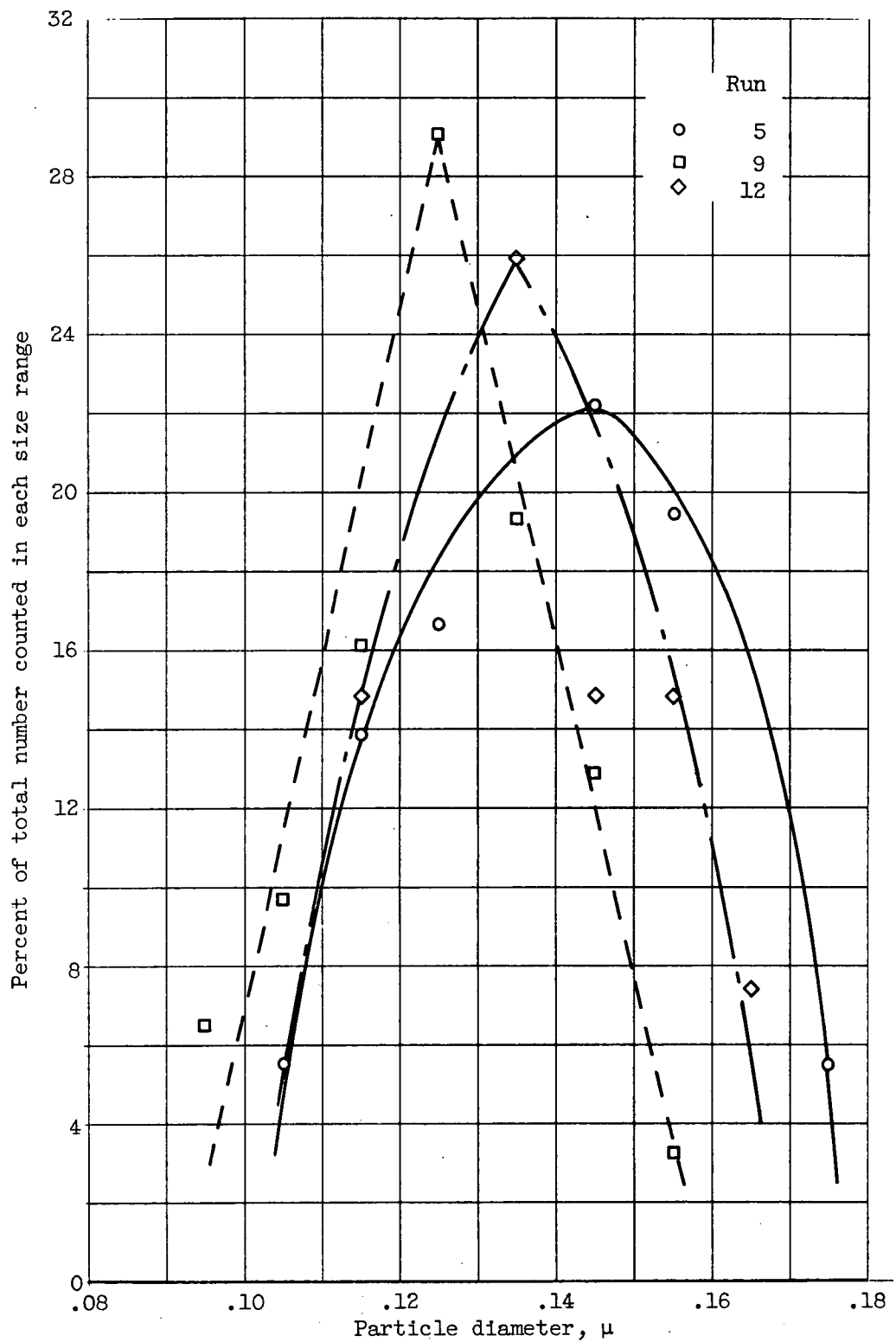


Figure 10. - Typical particle size distributions.

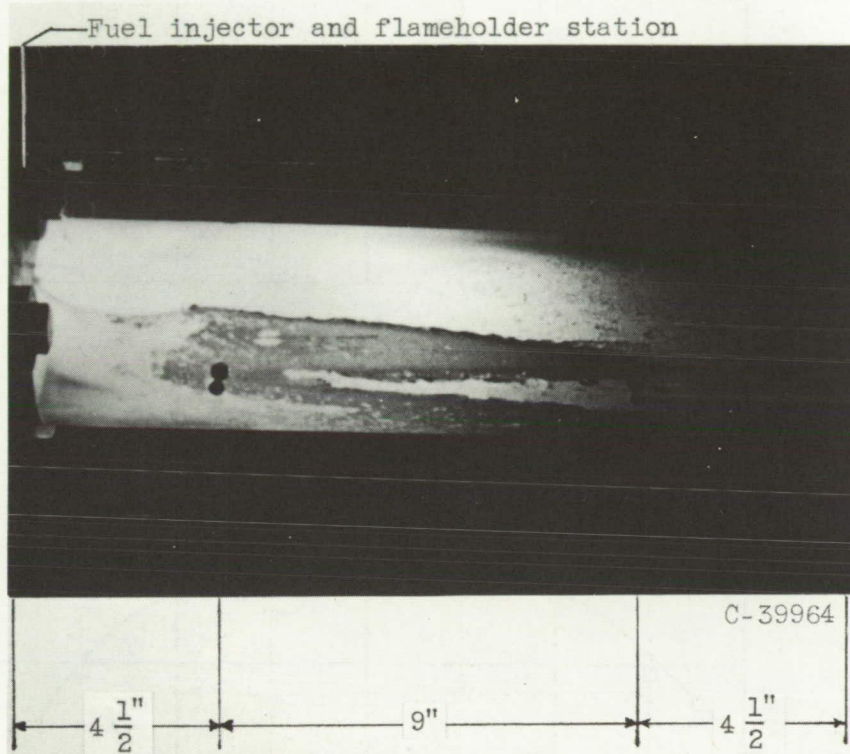


Figure 11. - Pentaborane flame through Lucite test section. Inlet-air velocity, 105 feet per second; equivalence ratio, 0.22.

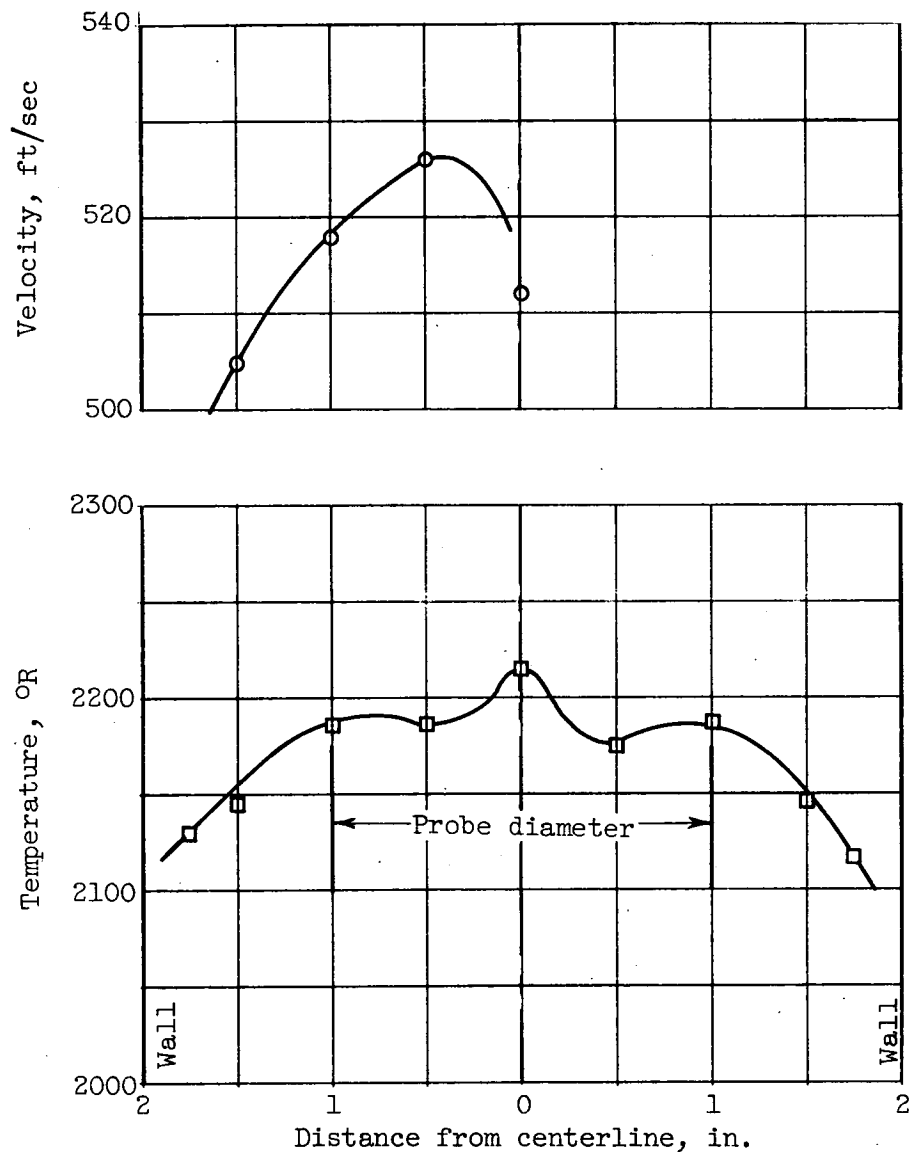


Figure 12. - Temperature and velocity profiles 22 inches from perforated plate. Run 2; equivalence ratio, 0.20.

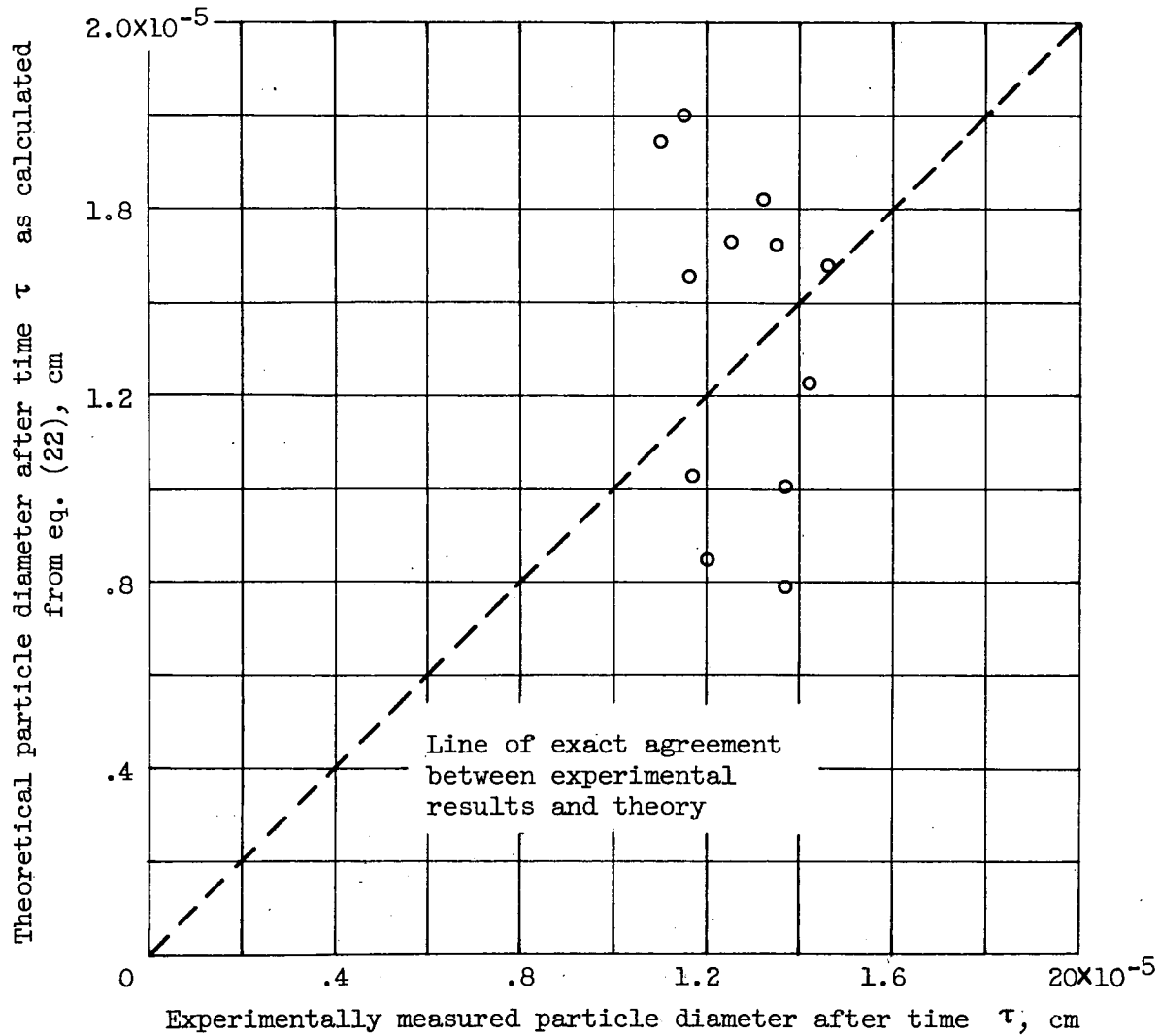


Figure 13. - Comparison of experimental results with equation (22).

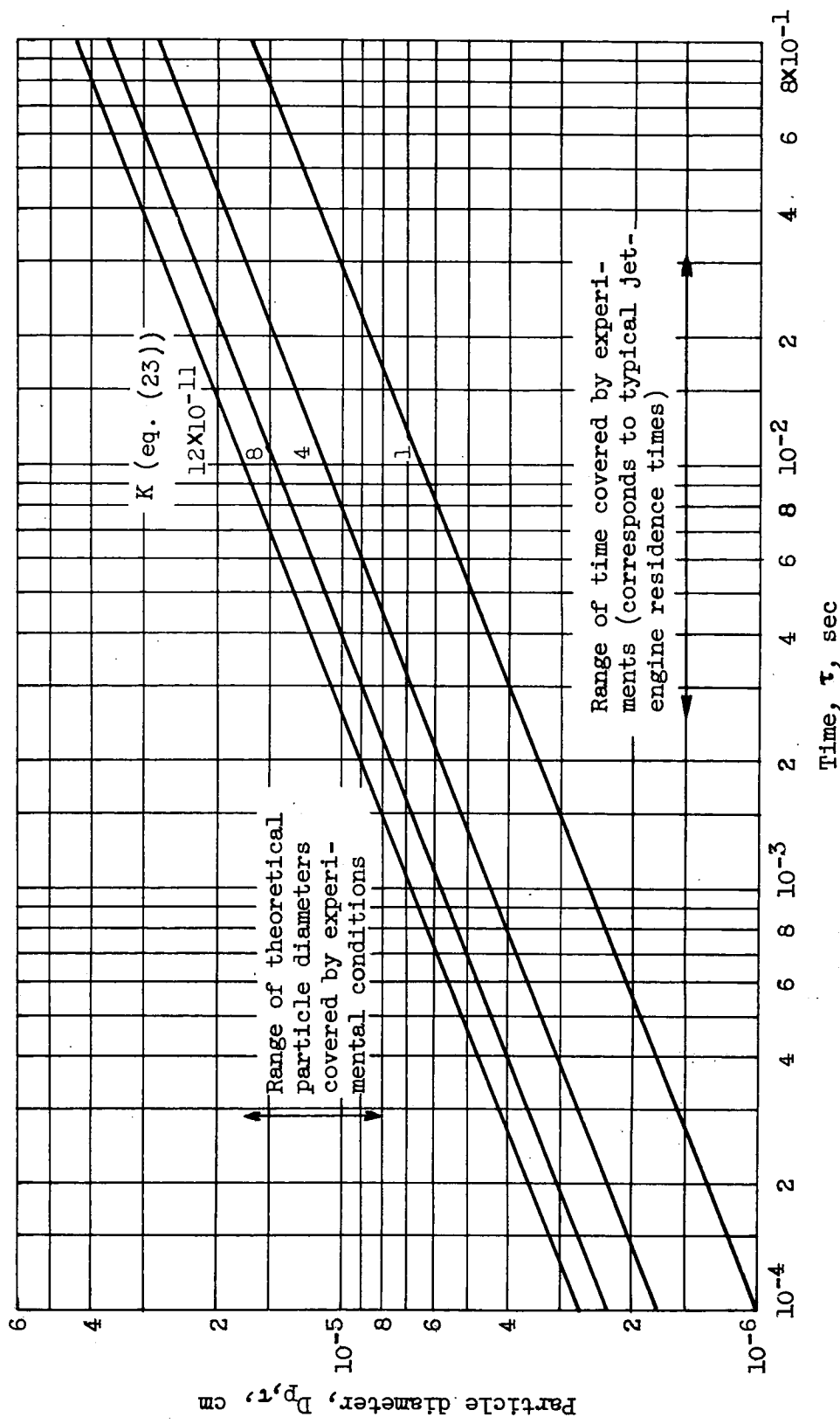


Figure 14. - Theoretical particle growth rates.

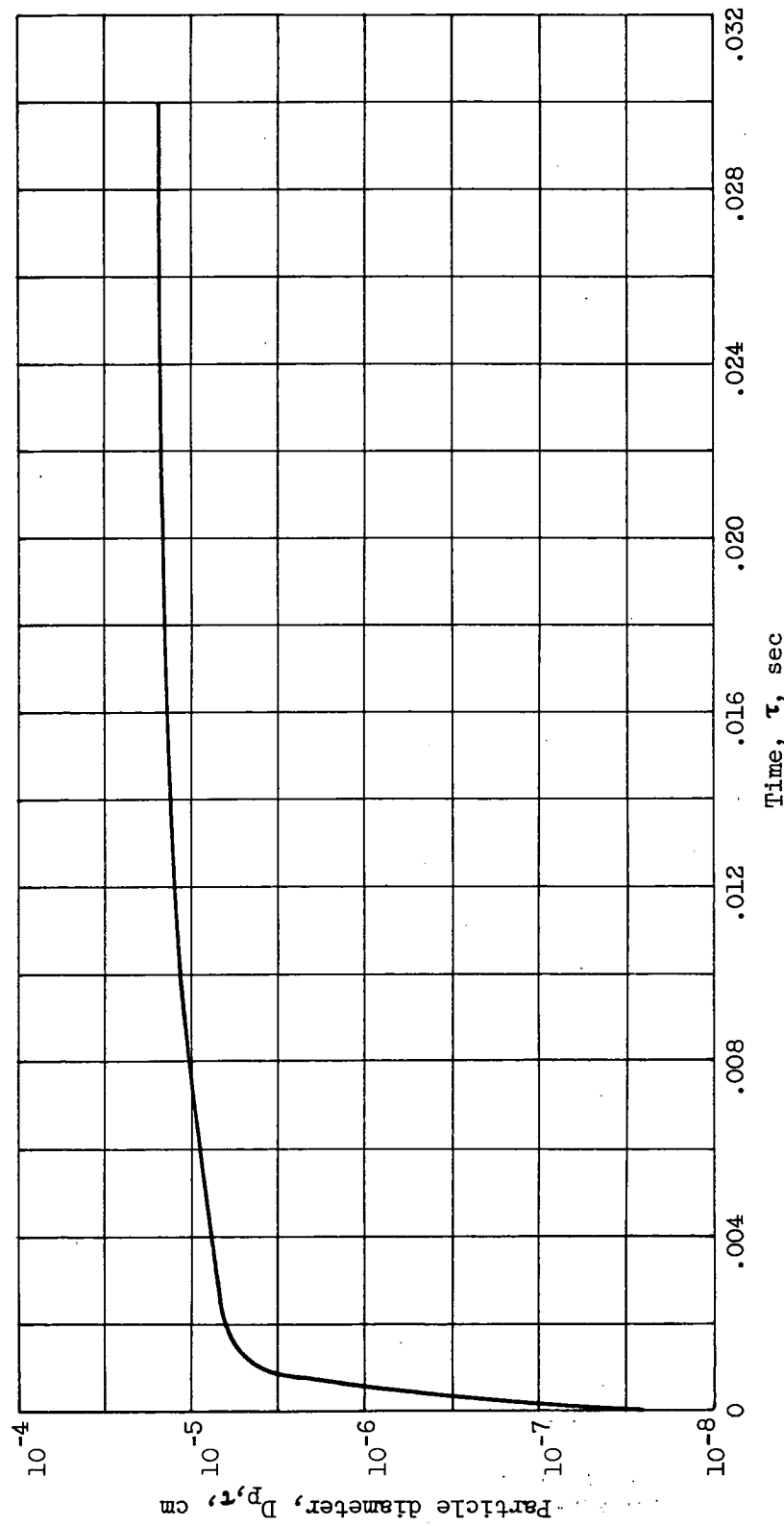


Figure 15. - Theoretical particle diameter as a function of growth time for $K = 4 \times 10^{-11}$.

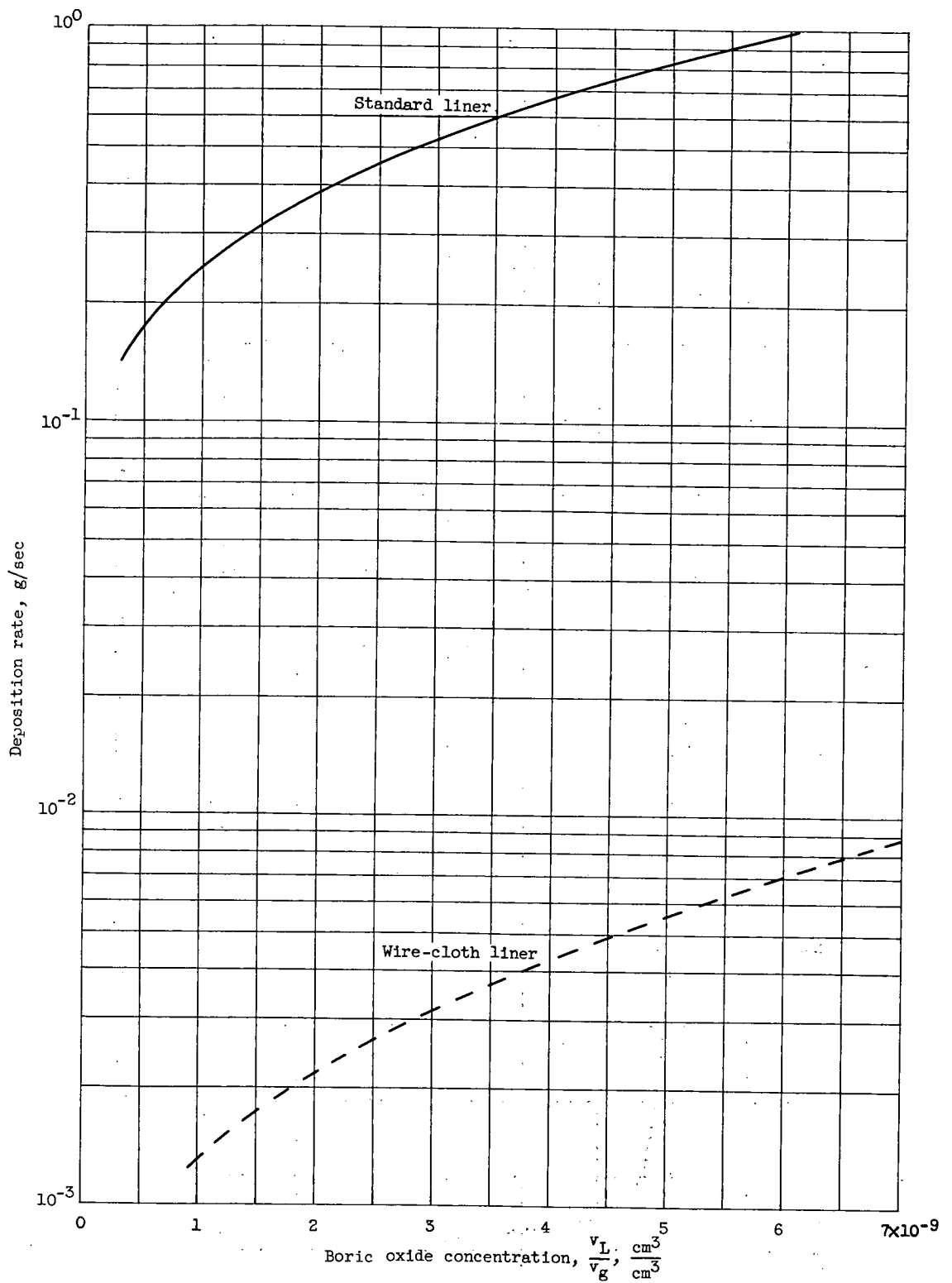


Figure 16. - Comparison of deposition rates of boric oxide on standard and wire-cloth combustor liners with pentaborane fuel.

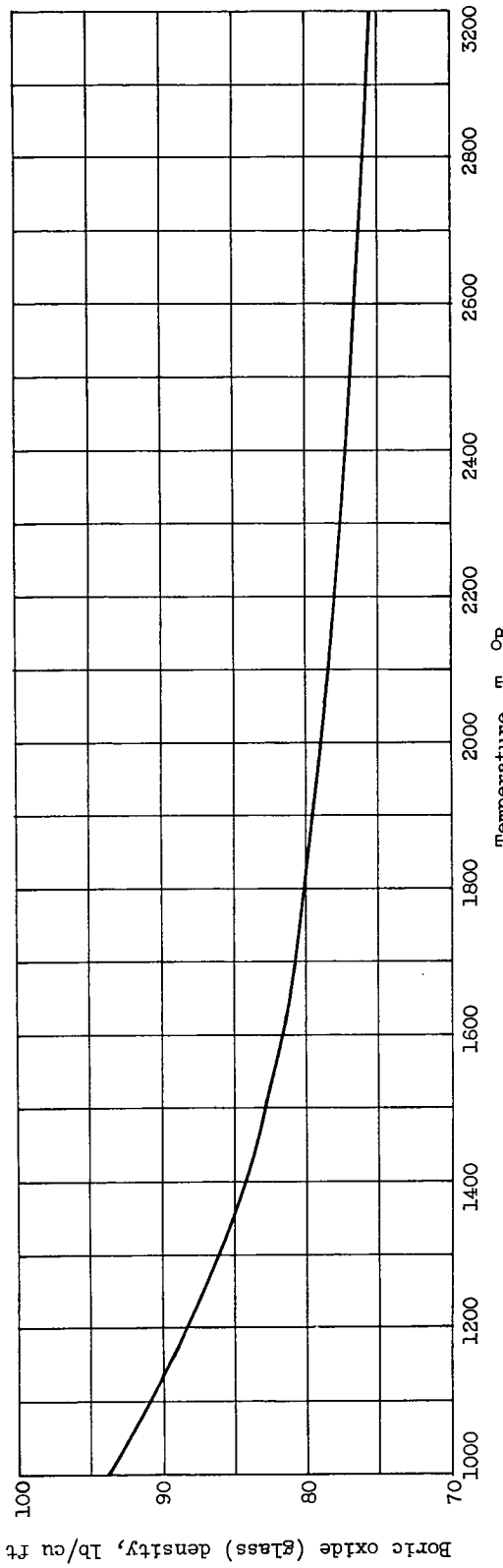


Figure 17. - Density of boric oxide as a function of temperature.